PCCP

ROYAL SOCIETY OF CHEMISTRY

PAPER

View Article Online
View Journal | View Issue

Cite this: *Phys. Chem. Chem. Phys.*, 2022, **24**, 2015

Vacuum ultraviolet photochemistry of sulfuric acid vapor: a combined experimental and theoretical study†

Cuihong Zhang,‡[abc] Xiaoxiao Lin,‡[a] Xiaofeng Tang,*[a] Christa Fittschen,[c] Sebastian Hartweg,[d] Gustavo A. Garcia,*[d] Bo Long,[e] Weijun Zhang[a] and Laurent Nahon[d]

Received 15th November 2021,
Accepted 20th December 2021

DOI: 10.1039/d1cp05237c

rsc.li/pccp

We present a vacuum ultraviolet (VUV) photoionization study of the gas-phase sulfuric acid (H_2SO_4) molecule in the 11–14 eV energy range by using the method of synchrotron radiation-based double imaging photoelectron photoion coincidence (i^2PEPICO) spectroscopy complemented with accurate theoretical calculations. The slow photoelectron spectrum (SPES) of H_2SO_4 has been acquired and the three electronic states of $H_2SO_4^+$, X^2A, A^2A and B^2A have been populated and assigned. The adiabatic ionization energy of the H_2SO_4 molecule towards the X^2A cationic ground state is measured at 11.684 ± 0.006 eV, in accordance with high-level calculated findings. With increasing photon energies, the $H_2SO_4^+$ cation dissociates into HSO_3^+ and OH fragments and their adiabatic appearance energy is measured at 13.498 ± 0.007 eV. Then, the enthalpies of formation for the species involved in the photoionization and dissociative photoionization have been determined through a thermochemical cycle.

1. Introduction

Sulfuric acid (H_2SO_4) as a key precursor plays an essential role in the formation of new particles, secondary aerosols and clouds in the earth's atmosphere, and has received much attention from both theoretical and experimental groups in recent years.[1–3] In the atmosphere, H_2SO_4 is mainly formed from the reaction of water vapor with sulfuric trioxide (SO_3), which is generated from the hydroxyl radical (OH) reaction with sulfuric dioxide (SO_2) emitted, for instance, from fossil fuel and biomass burning.[2,4,5] Due to its extremely low vapor pressure, the nascent H_2SO_4 molecule can easily get supersaturated and then enhance the homogenous nucleation rates of water and other compounds significantly. Presently, it is well-known that gas-phase H_2SO_4 molecules tend to form hydrates at the beginning of nucleation, that is, to produce small clusters consisting of a few water molecules associated with one or several H_2SO_4 molecules.[6–8] Thus, the structure and spectroscopy of H_2SO_4 and the sulfuric acid–water clusters are of considerable importance for understanding their chemistry in the atmosphere.

There have been several theoretical studies on H_2SO_4 and sulfuric acid–water clusters, in which their optimized structures and spectra have been calculated using various levels of theory.[9–12] For example, the theoretical results show that H_2SO_4 has two conformers depending on the relative position of the two OH groups: the most stable one is the *trans* form having a C_2 symmetry, while the *cis* form has a C_1 symmetry and an energy of +4.6 kJ mol^{-1} with respect to the *trans* conformer.[9] The energy barrier of isomerization was calculated to be 12.6 kJ mol^{-1} relative to the *trans* conformer.[9] Theoretical studies on the uptake of water molecules, leading to the hydration of H_2SO_4, have yielded the structure of these complexes, and it has been predicted that progressive hydration increases the probability of proton transfer from the acid to water, with the resulting ion-pair structures corresponding to the global energy minima.[9,11]

Experimentally, spectroscopic techniques such as microwave rotational spectroscopy, infrared (IR) spectroscopy and Raman spectroscopy have been employed to probe H_2SO_4 and hydrated complexes.[13–17] The structures, vibrational spectra and frequencies of H_2SO_4 and the $H_2SO_4{\cdot}H_2O$ cluster were

[a] *Laboratory of Atmospheric Physico-Chemistry, Anhui Institute of Optics and Fine Mechanics, HFIPS, Chinese Academy of Sciences, Hefei, 230031 Anhui, China. E-mail: tangxf@aiofm.ac.cn*
[b] *Graduate School, University of Science and Technology of China, Hefei, 230026 Anhui, China*
[c] *University Lille, CNRS, UMR 8522, PC2A – Physicochimie des Processus de Combustion et de l'Atmosphère, F-59000 Lille, France*
[d] *Synchrotron SOLEIL, L'Orme des Merisiers, St. Aubin BP 48, 91192 Gif sur Yvette, France. E-mail: gustavo.garcia@synchrotron-soleil.fr*
[e] *School of Materials Science and Engineering, Guizhou Minzu University, Guiyang, 550025 Guizhou, China*

† Electronic supplementary information (ESI) available. See DOI: 10.1039/d1cp05237c

‡ These authors contributed equally to this work.

obtained. Mass spectrometry, as a convenient analytical method, has also been applied in the past. For instance, the mass spectrum of H_2SO_4 vapor was acquired by Snow and Thomas using electron impact ionization mass spectrometry (EIMS) and its ionization energy was roughly measured at 12.4 eV, together with the appearance energies of its major fragment ions, H_2O^+, SO_3^+ and HSO_3^+.[18] The positive and negative ion distributions of the sulfuric acid–water clusters as well as their equilibrium constants were measured by Froyd and Lovejoy using EIMS.[19,20] Recently, the formation of mixed sulfuric acid–water clusters with different concentrations of water and H_2SO_4 has been investigated by electron attachment and negative ion mass spectrometry.[21] However, the above-mentioned mass spectrometry methods lack the energy resolution to distinguish contributions from all possible isomers. Moreover, much of the thermochemical data of H_2SO_4 and the sulfuric acid–water clusters are not precisely known.[22]

The purpose of this study is to investigate the vacuum ultraviolet (VUV) photodynamics of H_2SO_4. Photoionization and dissociative photoionization of H_2SO_4 in the energy range of 11–14 eV are analyzed by using the method of double imaging photoelectron photoion coincidence (i^2PEPICO) spectroscopy complemented with high-level theoretical calculations. Three cationic electronic states of $H_2SO_4^+$ have been prepared and assigned in the slow photoelectron spectrum (SPES). In particular, the adiabatic ionization energies (AIEs) of the *trans* and *cis* conformers of H_2SO_4, towards the X^2A cationic ground state, have been measured precisely for the first time, as well as the adiabatic appearance energy (AE_{0K}) of the HSO_3^+ fragment ion from the dissociation of $H_2SO_4^+$. The enthalpies of formation for the species involved in the photoionization and dissociative photoionization are also determined through a thermochemical cycle.

2. Materials and methods

The experiments were carried out on the beamline DESIRS equipped with an i^2PEPICO spectrometer, DELICIOUS III, at the French national synchrotron radiation facility SOLEIL. The detailed configurations of the synchrotron beamline and the spectrometer[23–25] have already been introduced in our previous publications and only a short description is presented here. Briefly, photons emitted from a variable polarization undulator were dispersed by a 6.65 m normal incidence monochromator equipped with a 200 L mm^{-1} grating, which was set to provide an energy resolution of $\sim$3 meV. A gas filter located upstream of the beamline and filled with Ar gas was employed to suppress high harmonics emitted from the undulator. The absolute photon energy of the beamline was calibrated online with a precision of $\pm$2.5 meV using the ionization energy of water.

The i^2PEPICO spectrometer is composed of a modified Wiley–McLaren ion time-of-flight (TOF) 3D-momentum imaging device and an electron velocity map imaging (VMI) analyzer, equipped with two position-sensitive detectors (PSDs) for the analysis of ions and electrons, respectively.[24] A mixture of helium carrier gas (1.5 bars), water vapor (from the vaporization of liquid water at room temperature) and H_2SO_4 vapor, generated from the vaporization of liquid H_2SO_4 (95% purity) in an in-vacuum oven heated at 180 °C, was expanded through a 70 μm diameter nozzle to form a continuous molecular beam which was skimmed twice before reaching the center of the spectrometer.[25,26] The multiplex coincidence scheme between the ion and electron yields mass-selected photoelectron spectra (PES) as a function of photon energy, which are then reduced to SPES, as previously detailed.[27,28] Meanwhile, the coincidence scheme can provide spectral fingerprints to identify and separate isomers, and accurately measure thermochemical data such as fragment appearance energies and bond energies.[29–31]

We have performed theoretical calculations to assign the experimental spectra. The AIE and the vertical ionization energy (VIE) of the X^2A ground electronic state of $H_2SO_4^+$ were calculated at the CCSD(T)-F12A/aug-cc-pVTZ level of theory as implemented in MOLPRO software.[32] The VIEs of the first (A^2A) and the second (B^2A) excited electronic states of $H_2SO_4^+$ were computed using time-dependent density functional theory (TD-DFT), TD-M062X/6-311++G(d,p).[33] The Franck–Condon factors in the photoionization towards the X^2A cationic ground state, as well as for the required geometry optimizations and the vibrational frequency computations with a harmonic approximation, were calculated at the M062X/6-311++G(d,p) level of theory with the Gaussian package using the time-independent adiabatic Hessian Franck–Condon model.[33]

3. Results and discussion

3.1 TOF mass spectra

Synchrotron radiation photoionization TOF mass spectra of the gas mixture have been recorded in the 11–14 eV photon energy range and are presented as a matrix in Fig. 1, as well as their integrated mass spectra. Several mass peaks can be observed and have been assigned within a mass range of m/z = 60–110. For example, the most intense mass peak at m/z = 98 is assigned to H_2SO_4, the m/z = 80 mass peak is assigned to SO_3 and the m/z = 64 peak is attributed to SO_2, based on their narrow widths in the mass spectra.[25] Indeed, the width of the TOF peak is proportional to the square root of the ion translational energy along the detection axis, so that narrow peaks correspond to parent ions formed by direct ionization of the neutrals in the molecular beam, while broad peaks originate from fragment ions formed by dissociative ionization.[25,30] Besides these three intense mass peaks, their isotopic peaks can be observed in the mass spectra too, *i.e.*, the $^{33}SO_2$ isotopic species at m/z = 65, $^{34}SO_2$ at m/z = 66, $^{34}SO_3$ at m/z = 82 and $H_2{}^{34}SO_4$ at m/z = 100 with relative intensities corresponding to their individual natural abundances, as listed in Table S1 (ESI†).[34]

SO_3 is formed from the equilibrium reaction of $H_2SO_4(g) \leftrightarrow SO_3(g) + H_2O(g)$ inside the oven, and SO_2 is produced from the reduction reaction of H_2SO_4 with the metallic parts of the oven. The appearance energies of SO_3 and SO_2 can be obtained from

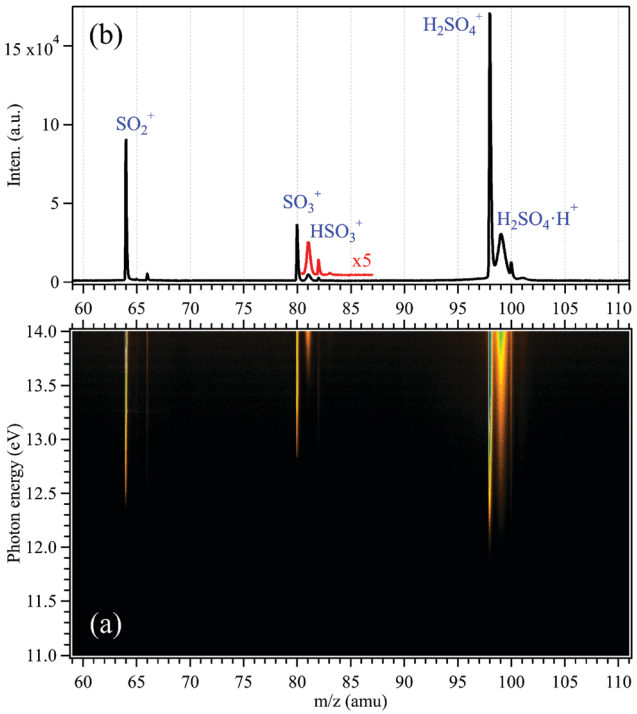

Fig. 1 (a) Synchrotron photoionization mass spectra matrix in the 11–14 eV energy range and (b) their integrated mass spectrum, together with 5 times magnified data in red.

the mass spectra matrix of Fig. 1(a) and both of them agree with their individual ionization energies,[35] confirming their assignments as neutral nascent species formed in the oven. Note that SO_3^+ and SO_2^+ were also observed in a previous study based on EIMS, but both were assigned as fragment ions from the dissociation of $H_2SO_4^+$ by Snow and Thomas.[18]

Normally, in Fig. 1, the mass peak at m/z = 81 should be assigned as the $^{33}SO_3$ isotopic species in the mass spectra. But, its relative intensity (~28% of $^{32}SO_3$) measured in the mass spectrum is much higher than the natural abundance of $^{33}SO_3$ (~0.91%),[34] and its peak width is much wider than that of the SO_3 or H_2SO_4 mass peak. In addition, as shown in the mass spectra matrix, the appearance energy of the m/z = 81 species is not the same as and much higher than that of SO_3 (m/z = 80). Therefore, the m/z = 81 peak in the mass spectra is not contributed from the isotope $^{33}SO_3$ and corresponds to the HSO_3^+ fragment ion from the dissociative ionization of H_2SO_4, as inferred from its broad shape due to the kinetic energy release in the fragmentation. Note that the contribution from the isotope $^{33}SO_3$ (~0.91%)[34] to the m/z = 81 channel is considered negligible and has not been subtracted here. Similarly, due to its large width, the more intense peak at m/z = 99 is attributed to the $H_2SO_4H^+$ fragment ion produced from the dissociative photoionization of the $H_2SO_4 \cdot H_2O$ complexes formed in the molecular beam, with again a negligible contribution from the $H_2{}^{33}SO_4^+$ isotopic species. Note that a complete study of water complexes and clusters of sulfuric acid will be reported in a forthcoming work.

3.2 Mass-selected slow photoelectron spectra

The mass-selected photoelectron matrices corresponding to the $H_2SO_4^+$ parent ion (m/z = 98) and the HSO_3^+ fragment ion (m/z = 81) showing the signal as a function of electron kinetic energy (Ele KE) and photon energy are depicted in Fig. 2(a and c), respectively. Here, diagonal lines are the product of energy conservation and thus correspond to constant cationic states.

The mass-selected SPES corresponding to the $H_2SO_4^+$ parent ion and the HSO_3^+ fragment ion are obtained from the photoelectron matrices and presented in Fig. 2(b and d), respectively,

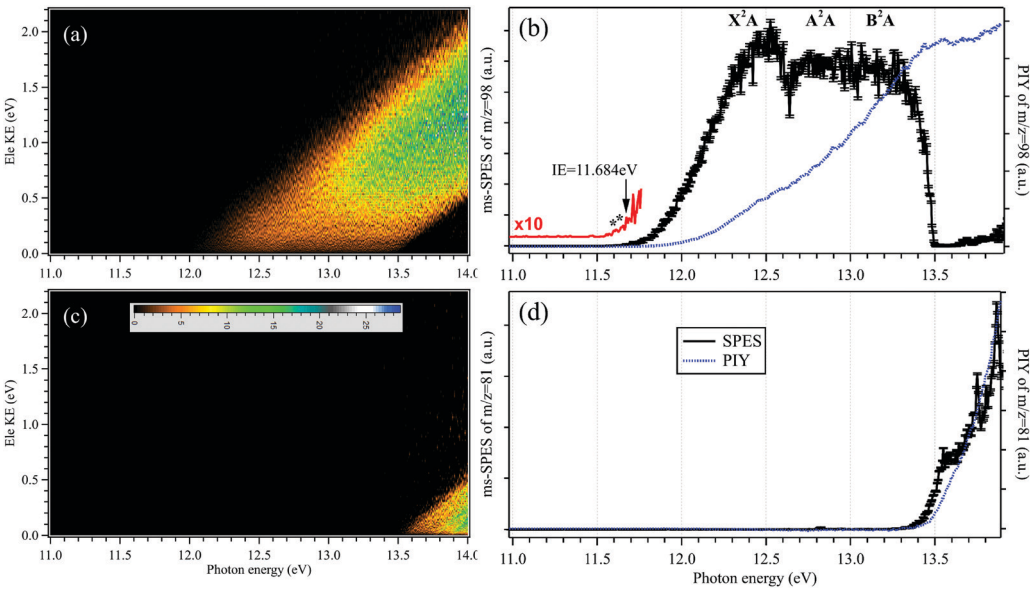

Fig. 2 Mass-selected photoelectron matrices, slow photoelectron spectra (SPES, black solid lines) and photoionization yields (PIYs, blue dotted lines) corresponding to (a and b) the $H_2SO_4^+$ parent ion and (c and d) the HSO_3^+ fragment ion. The 10 times magnified SPES in red shows the onset of $H_2SO_4^+$.

as well as their photoionization yields (PIYs).[27,28] In Fig. 2(b), the SPES of H_2SO_4 is rather unstructured although an onset can be observed at $h\nu$ = 11.684 ± 0.006 eV in the SPES. The uncertainty of the photon energy calibration, the influence of the scanning step size (5 meV) and the signal-to-noise ratio of the SPES have been taken into account and included in the given error bars.[36]

As mentioned in the introduction, the gas-phase H_2SO_4 molecule has two conformers, *trans* and *cis*, and their optimized structures as the neutrals as well as their cations in the X^2A cationic ground state have been calculated and are presented in Fig. 3, agreeing well with previous results.[9,37] The *trans* conformer has a C_2 symmetry structure and is the global minimum with an energy of ~4.6 kJ mol^{-1} below the *cis* conformer with a C_1 symmetry.[9] The temperature of the molecules in the molecular beam is estimated at 150 K (see Section 3.3 below), which would mean that the *trans* conformer is dominant, with only ~2% for the *cis* conformer. However, the flash cooling in the adiabatic expansion might lead to a different conformer population than the one expected assuming thermal equilibrium.

Upon photoionization, an electron is removed from the outer valence orbital of the neutral H_2SO_4 molecule leading to the formation of the $H_2SO_4^+$ cation. The structure of the *trans* conformer relaxes in the cation and its symmetry changes from C_2 to C_1 during the photoionization, as shown in Fig. 3, while the *cis* conformer geometry undergoes smaller changes. The AIE of the X^2A ground electronic state of the *trans*-$H_2SO_4^+$ has been calculated at 11.688 eV using the CCSD(T)-F12A/aug-cc-pVTZ method with zero-point corrections (ZPEs).[32] Note that no scaling factor has been used for the determination of harmonic frequencies and ZPEs. The calculated values are consistent with the onset of the experimental curve and their differences are within 10 meV. Although some structures are seen in the region where the AIEs are predicted in our experimental spectra, the unfavorable Franck–Condon factors and consequent lack of structure do not allow a definite assignment of the experimental AIE. Nevertheless, in view of the good agreement between the calculated AIE and the feature at 11.684 eV, we tentatively offer this value as the AIE of the *trans* conformer. The very weak features at 11.643 and 11.609 eV (marked with two asterisks in the 10 times magnified data of Fig. 2b) might be ascribed to the *cis* conformer, with the former being assigned to the AIE of the X^2A ground state, for which the value is calculated at 11.635 eV, and the latter originating from a hot band in the photoionization, *i.e.*, from the v_2 vibrational mode of the *cis* conformer whose frequency is calculated at 289.32 cm^{-1} using the M062X/6-311++G(d,p) method. However, we note that purely thermal arguments would not allow for the presence of the *cis* conformer, nor a hot band, at the presently estimated temperature of 150 K. In a previous study based on EIMS, restricted by the electron energy resolution, the ionization energy of H_2SO_4 was measured at 12.4 ± 0.05 eV (see Table 1), which would actually correspond to the VIE measured in this work.[18]

The Franck–Condon factors for the photoionization of H_2SO_4 towards the cationic X^2A ground electron state of $H_2SO_4^+$ have been calculated at the M062X/6-311++G(d,p) level of theory, using the time-independent adiabatic Hessian Franck–Condon model.[33] Note that the influences of inconsequential internal rotations are not included in this model and thus, the differences of the two conformers are not considered in the Franck–Condon factors. The simulated PES is subsequently generated by convolving the stick spectrum with a Gaussian function (FWHM = 100 cm^{-1}, full width at half maximum) and is shown in Fig. S1 (ESI†), with an energy offset of 50 meV to fit the experimental result. Although the simulated PES fits the experimental SPES very well at the beginning of the X^2A state, an apparent difference can be observed between them at the high energy part, indicating that other factors need to be considered, such as the appearance of cationic excited electronic states. Indeed, the VIEs of the A^2A excited electronic state and the B^2A electronic state of $H_2SO_4^+$ have been calculated at 12.84 and 13.10 eV, respectively, at the TD-M062X/6-311++G(d,p) level of theory, and have been assigned in the experimental SPES too. In the SPES of Fig. 2(b), the VIEs of the A^2A and B^2A cationic states are estimated at 12.80 ± 0.05 and

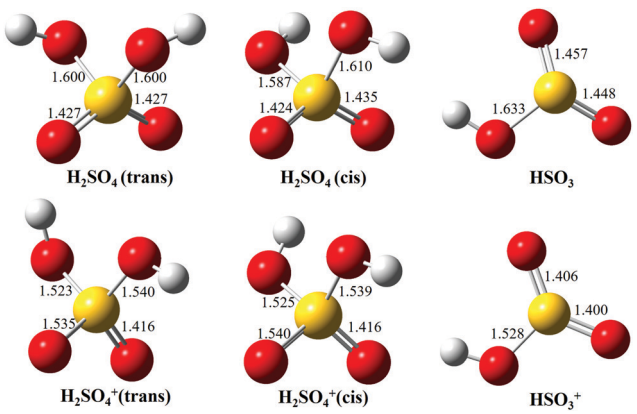

Fig. 3 Optimized structures of H_2SO_4 (*trans* and *cis* conformers) and HSO_3, as well as their individual cations, in the ground electronic states.

Table 1 Ionization energies of H_2SO_4 and the appearance energy of the HSO_3^+ fragment ion (unit: eV).

	State	IE(H_2SO_4)	AE(HSO_3^+)	Method	Ref.
Expt.		12.4 ± 0.05		EIMS	18
			13.9 ± 0.1	EIMS	18
			13.498 ± 0.007	SPES	*e*
	X^2A (*trans*)	11.684 ± 0.006[a]		SPES	*e*
	X^2A (*cis*)	11.643 ± 0.006[a]		SPES	*e*
	X^2A	12.53 ± 0.05[b]		SPES	*e*
	A^2A	12.80 ± 0.05[b]		SPES	*e*
	B^2A	13.20 ± 0.05[b]		SPES	*e*
Calc.	X^2A (*trans*)	11.688[a]		CCSD(T)[c]	*e*
	X^2A (*cis*)	11.635[a]		CCSD(T)[c]	*e*
	X^2A	12.54[b]		CCSD(T)[c]	*e*
	A^2A	12.84[b]		TD-M062X[d]	*e*
	B^2A	13.10[b]		TD-M062X[d]	*e*

[a] AIE. [b] VIE. [c] CCSD(T)-F12A/aug-cc-pVTZ. [d] TD-M062X/6-311+ +G(d,p). [e] This work.

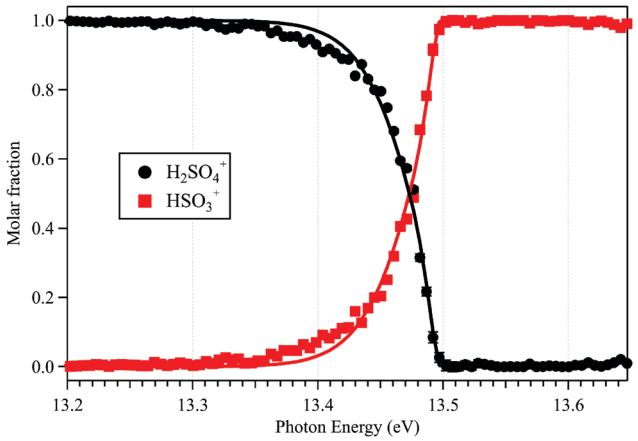

Fig. 4 Breakdown diagram of the $H_2SO_4^+$ parent ion (m/z = 98) and HSO_3^+ fragment ion (m/z = 81). Solid circles represent the experimental data, while lines correspond to the statistical model (see text for details).

13.20 ± 0.05 eV, respectively, as listed in Table 1, agreeing well with the calculated results.

3.3 The thermochemical cycle

The sharp high energy cut-off of the electron signal in the parent SPES of Fig. 2(b) is due to the dissociative photoionization of H_2SO_4, in accordance with the sharp appearance of the electron signal in the SPES of the HSO_3^+ fragment ion in Fig. 2(d). The HSO_3^+ fragment ion was also observed in the electron impact ionization mass spectra of Snow and Thomas, and its appearance energy was measured at 13.9 ± 0.1 eV.[18] Fig. 4 presents the breakdown diagram of the sulfuric acid cation, showing the molar fractions of the unimolecular reaction $H_2SO_4^+ \rightarrow HSO_3^+ + OH$ as a function of the photon energy, as extracted from the parent and fragment SPES in Fig. 2. The curves in the breakdown diagram can be modelled assuming that the initial internal thermal energy stored in the parent neutral molecule can be directed towards fragmentation.[38] Assuming that dissociation is fast within the acceleration timescales of the experimental setup (a few microseconds), the only parameters affecting the model are the temperature and the 0 K appearance energy of the HSO_3^+ fragment. These are optimized within a least squares fit to the data which yields values of 150 ± 20 K for the temperature, and $AE_{0K}(HSO_3^+)$ = 13.498 ± 0.007 eV, very far from the data reported by Snow and Thomas. Note that we cannot resolve contributions from *cis* and *trans* conformers in the breakdown diagram, so that we assume that the same AE_{0K} applies to both, *i.e.*, that the eventual barriers towards dissociation are equal.

Based on the AIE of the X^2A ground state of $H_2SO_4^+$ and the AE_{0K} of the HSO_3^+ fragment ion, the bond energy of $H_2SO_4^+$ associated with the HSO_3^+ and OH fragments is calculated at 1.814 ± 0.008 eV for the *trans* conformer. Through a thermochemical cycle, as shown in Fig. 5, the enthalpies of formation for the cations of $H_2SO_4^+$ and HSO_3^+ are obtained at $\Delta_fH_{0K}(H_2SO_4^+)$ = 406.2 ± 8.5 kJ mol^{-1} and $\Delta_fH_{0K}(HSO_3^+)$ = 543.9 ± 8.5 kJ mol^{-1}, with the aid of the available

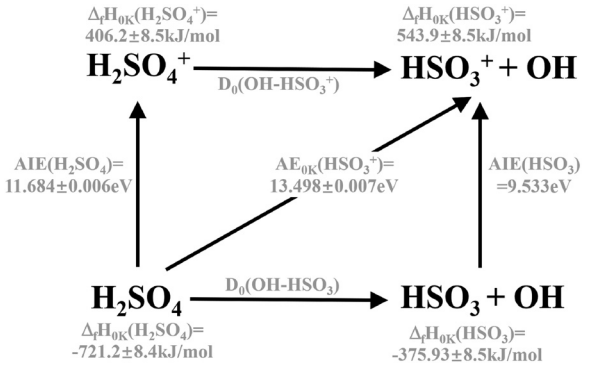

Fig. 5 The thermochemical cycle in photoionization and dissociative photoionization of H_2SO_4.

thermochemical data in the literature, *i.e.*, $\Delta_fH_{0K}(H_2SO_4)$ = −721.2 ± 8.4 kJ mol^{-1} [39] and $\Delta_fH_{0K}(OH)$ = 37.252 ± 0.026 kJ mol^{-1},[40] and assuming barrierless fragmentations. In addition, the AIE of the HSO_3 radical is calculated at 9.533 eV with the CCSD(T)-F12A/aug-cc-pVTZ high-level of theory,[32] so that we report the enthalpy of formation for HSO_3 at $\Delta_fH_{0K}(HSO_3)$ = −375.9 ± 8.5 kJ mol^{-1}.

4. Conclusions

In summary, VUV photoionization and dissociative photoionization of H_2SO_4 in the 11–14 eV energy range have been investigated by using the i^2PEPICO technique complemented with accurate theoretical calculations on the structures and ionization energies. The H_2SO_4 molecule in the oven is seen to decompose to form SO_2 and SO_3 and these can be discarded by the coincidence scheme and are distinguished from the dissociative ionization product, the HSO_3^+ fragment ion. The "pure" high-resolution SPES of H_2SO_4 without contaminations from other species in the continuous molecular beam has been acquired for the first time. The three cationic electronic states, $H_2SO_4^+$, X^2A, A^2A and B^2A, are observed and assigned in the SPES, with the aid of the high-level theoretical calculated results. The H_2SO_4 molecule has two conformers, *trans* and *cis*, and their individual AIEs of the X^2A cationic ground state have been tentatively measured at 11.684 ± 0.006 and 11.643 ± 0.006 eV, respectively. The VIEs of the three electronic states are also determined. With increasing photon energies, the $H_2SO_4^+$ cation dissociates into the HSO_3^+ and OH fragments and their adiabatic appearance energy is measured at 13.498 ± 0.007 eV. Furthermore, the enthalpies of formation for the cations $H_2SO_4^+$ and HSO_3^+ are acquired through the thermochemical cycle in the photoionization and dissociative photoionization.

Author contributions

Cuihong Zhang: investigation; Xiaoxiao Lin: formal analysis; Xiaofeng Tang: conceptualization, methodology, investigation, project administration, writing – original draft, and writing – review and editing. Christa Fittschen: investigation; Sebastian

Hartweg: investigation; Gustavo A. Garcia: methodology, data curation, investigation, writing – original draft, and writing – review and editing; Bo Long: formal analysis; Weijun Zhang: formal analysis; Laurent Nahon: methodology, investigation, and writing – review and editing.

Conflicts of interest

There are no conflicts to declare.

Acknowledgements

X. T. would like to acknowledge the financial support from the National Natural Science Foundation of China (No. 91961123, 21773249 and 42120104007), the International Partnership Program of the Chinese Academy of Sciences (No. 116134KYSB20170048) and the Key Program of Research and Development of Hefei Science Center, CAS (No. 2020HSCKPRD001). C. Z. thanks the Chinese Scholarship Council for financial support (No. 202006340125). C. F. acknowledges the support from the Chinese Academy of Sciences President's International Fellowship Initiative (No. 2018VMA0055). B. L. is grateful to the Science and Technology Foundation of Guizhou Province (No. [2019]5648), and the Science and Technology Foundation of Guizhou Provincial Department of Education, China (No. KY[2021]014). The authors are grateful to the SOLEIL general staff for smoothly running the facility and providing synchrotron beamtime under the proposal 20200490. In particular, Jean-François Gil is warmly thanked for his help in setting up the experiment.

References

1 M. Sipila, T. Berndt, T. Petaja, D. Brus and J. Vanhanen, *et al.*, The role of sulfuric acid in atmospheric nucleation, *Science*, 2010, **327**, 1243–1246.
2 T. Berndt, O. Boge, F. Stratmann, J. Heintzenberg and M. Kulmala, Rapid formation of sulfuric acid particles at near-atmospheric conditions, *Science*, 2005, **307**, 698–700.
3 M. Torrent-Sucarrat, J. S. Francisco and J. M. Anglada, Sulfuric acid as autocatalyst in the formation of sulfuric acid, *J. Am. Chem. Soc.*, 2012, **134**, 20632–20644.
4 B. Long, Z.-W. Long, Y.-B. Wang, X.-F. Tan and Y.-H. Han, *et al.*, Formic acid catalyzed gas-phase reaction of H_2O with SO_3 and the reverse reaction: a theoretical study, *ChemPhysChem*, 2012, **13**, 323–329.
5 B. Long, J. L. Bao and D. G. Truhlar, Reaction of SO_2 with OH in the atmosphere, *Phys. Chem. Chem. Phys.*, 2017, **19**, 8091–8100.
6 D. R. Hanson and E. R. Lovejoy, Measurement of the thermodynamics of the hydrated dimer and trimer of sulfuric acid, *J. Phys. Chem. A*, 2006, **110**, 9525–9528.
7 B. Temelso, T. E. Morrell, R. M. Shields, M. A. Allodi and E. K. Wood, *et al.*, Quantum mechanical study of sulfuric acid hydration: atmospheric implications, *J. Phys. Chem. A*, 2012, **116**, 2209–2224.
8 E. R. Lovejoy, J. Curtius and K. D. Froyd, Atmospheric ion-induced nucleation of sulfuric acid and water, *J. Geophys. Res.: Atmos.*, 2004, **109**, D08204.
9 S. Re, Y. Osamura and K. Morokuma, Coexistence of neutral and ion-pair clusters of hydrated sulfuric acid $H_2SO_4(H_2O)_n$ (n = 1–5) – A molecular orbital study, *J. Phys. Chem. A*, 1999, **103**, 3535–3547.
10 V. Loukonen, T. Kurten, I. K. Ortega, H. Vehkamaki and A. A. H. Padua, *et al.*, Enhancing effect of dimethylamine in sulfuric acid nucleation in the presence of water – a computational study, *Atmos. Chem. Phys.*, 2010, **10**, 4961–4974.
11 B. Temelso, P. Thuong Ngoc and G. C. Shields, Computational study of the hydration of sulfuric acid dimers: implications for acid dissociation and aerosol formation, *J. Phys. Chem. A*, 2012, **116**, 9745–9758.
12 Y. Miller, G. M. Chaban and R. B. Gerber, *Ab initio* vibrational calculations for H_2SO_4 and H_2SO_4 H_2O: spectroscopy and the nature of the anharmonic couplings, *J. Phys. Chem. A*, 2005, **109**, 6565–6574.
13 P. A. Giguere and R. Savoie, The normal vibrational frequencies and the thermodynamic functions of H_2SO_4 and D_2SO_4, *J. Am. Chem. Soc.*, 1963, **85**, 287–289.
14 K. L. Nash, K. J. Sully and A. B. Horn, Observations on the interpretation and analysis of sulfuric acid hydrate infrared spectra, *J. Phys. Chem. A*, 2001, **105**, 9422–9426.
15 C. E. L. Myhre, D. H. Christensen, F. M. Nicolaisen and C. J. Nielsen, Spectroscopic study of aqueous H_2SO_4 at different temperatures and compositions: variations in dissociation and optical properties, *J. Phys. Chem. A*, 2003, **107**, 1979–1991.
16 A. Givan, L. A. Larsen, A. Loewenschuss and C. J. Nielsen, Infrared matrix isolation study of H_2SO_4 and its complexes with H_2O, *J. Chem. Soc., Faraday Trans.*, 1998, **94**, 827–835.
17 D. L. Fiacco, S. W. Hunt and K. R. Leopold, Microwave investigation of sulfuric acid monohydrate, *J. Am. Chem. Soc.*, 2002, **124**, 4504–4511.
18 K. B. Snow and T. F. Thomas, Mass spectrum, ionization potential, and appearance potentials for fragment ions of sulfuric acid vapor, *Int. J. Mass Spectrom. Ion Processes*, 1990, **96**, 49–68.
19 K. D. Froyd and E. R. Lovejoy, Experimental thermodynamics of cluster ions composed of H_2SO_4 and H_2O. 1. positive ions, *J. Phys. Chem. A*, 2003, **107**, 9800–9811.
20 K. D. Froyd and E. R. Lovejoy, Experimental thermodynamics of cluster ions composed of H_2SO_4 and H_2O. 2. measurements and *ab initio* structures of negative ions, *J. Phys. Chem. A*, 2003, **107**, 9812–9824.
21 J. Lengyel, A. Pysanenko and M. Farnik, Electron-induced chemistry in microhydrated sulfuric acid clusters, *Atmos. Chem. Phys.*, 2017, **17**, 14171–14180.
22 K. Do, T. P. Klein, C. A. Pommerening, S. M. Bachrach and L. S. Sunderlin, The gas-phase basicity of sulfuric acid, *J. Am. Chem. Soc.*, 1998, **120**, 6093–6096.
23 L. Nahon, N. de Oliveira, G. A. Garcia, J. F. Gil and B. Pilette, *et al.*, DESIRS: a state-of-the-art VUV beamline featuring high resolution and variable polarization for spectroscopy

and dichroism at SOLEIL, *J. Synchrotron Radiat.*, 2012, **19**, 508–520.
24 G. A. Garcia, B. K. C. de Miranda, M. Tia, S. Daly and L. Nahon, Delicious III: A multipurpose double imaging particle coincidence spectrometer for gas phase vacuum ultraviolet photodynamics studies, *Rev. Sci. Instrum.*, 2013, **84**, 053112.
25 X. Tang, G. A. Garcia, J. F. Gil and L. Nahon, Vacuum upgrade and enhanced performances of the double imaging electron/ion coincidence end-station at the vacuum ultraviolet beamline DESIRS, *Rev. Sci. Instrum.*, 2015, **86**, 123108.
26 S. Hartweg, G. A. Garcia and L. Nahon, Photoelectron spectroscopy of the water dimer reveals unpredicted vibrational structure, *J. Phys. Chem. A*, 2021, **125**, 4882–4887.
27 J. C. Poully, J. P. Schermann, N. Nieuwjaer, F. Lecomte and G. Gregoire, *et al.*, Photoionization of 2-pyridone and 2-hydroxypyridine, *Phys. Chem. Chem. Phys.*, 2010, **12**, 3566–3572.
28 M. Briant, L. Poisson, M. Hochlaf, P. de Pujo and M.-A. Gaveau, *et al.*, Ar_2 photoelectron spectroscopy mediated by autoionizing states, *Phys. Rev. Lett.*, 2012, **109**, 193401.
29 X. Tang, X. Lin, G. A. Garcia, J.-C. Loison and Z. Gouid, *et al.*, Identifying isomers of peroxy radicals in the gas phase: 1-$C_3H_7O_2$ vs. 2-$C_3H_7O_2$, *Chem. Commun.*, 2020, **56**, 15525–15528.
30 X. Tang, G. A. Garcia and L. Nahon, High-resolution vacuum ultraviolet photodynamic of the nitrogen dioxide dimer $(NO_2)_2$ and the stability of its cation, *Phys. Chem. Chem. Phys.*, 2020, **22**, 21068–21073.
31 K. Voronova, K. M. Ervin, K. G. Torma, P. Hemberger and A. Bodi, *et al.*, Radical thermometers, thermochemistry, and photoelectron spectra: a photoelectron photoion coincidence spectroscopy study of the methyl peroxy radical, *J. Phys. Chem. Lett.*, 2018, **9**, 534–539.
32 H.-J. Werner and P. J. Knowles, *MOLPRO version*, 2015, http://www.molpro.net.
33 M. J. Frisch, G. W. Trucks, H. B. Schlegel, G. E. Scuseria and M. A. Robb, *et al.*, *Gaussian 09, Revision A02*, Gaussian, Inc., Wallingford CT, 2016.
34 K. J. R. Rosman and P. D. P. Taylor, Isotopic compositions of the elements 1997, *J. Anal. At. Spectrom.*, 1999, **14**, 5N–24N.
35 NIST Chemistry WebBook, http://webbook.nist.gov/chemistry/, Accessed October 21, 2021.
36 J. W. Brault, High precision Fourier transform spectrometry: The critical role of phase corrections, *Microchim. Acta*, 1987, **3**, 215–227.
37 C. G. Ding, K. Laasonen and A. Laaksonen, Two sulfuric acids in small water clusters, *J. Phys. Chem. A*, 2003, **107**, 8648–8658.
38 B. Sztaray, A. Bodi and T. Baer, Modeling unimolecular reactions in photoelectron photoion coincidence experiments, *J. Mass Spectrom.*, 2010, **45**, 1233–1245.
39 M. W. Chase, Jr., *NIST-JANAF Thermochemical Tables*, 4th edn, 1998, pp. 1–1951, https://janaf.nist.gov.
40 B. Ruscic and D. H. Bross, Active thermochemical tables (ATcT) values based on ver. 1.122 g of the thermochemical network (2019); available at https://ATcT.anl.gov (accessed 24th of October 2021).